

Coastal Ocean Observatories Enable Biological Investigations in a Buoyant Plume

Frazer, T.K.; Keller, S.R.

University of Florida, Department of Fisheries and Aquatic Sciences, 7922 NW 71st Street, Gainesville, FL, 32653, USA
(frazer@ufl.edu, srk2@ufl.edu)

Schofield, O.; Glenn, S.M.; Kohut, J.; Chant, R.J.; Oliver, M.; Reinfelder, J.R.;

Rutgers University, 71 Dudley Road, New Brunswick, NJ, 08901, USA

(oscar@marine.rutgers.edu, glenn@caribbean.rutgers.edu, kohut@marine.rutgers.edu, chant@imcs.rutgers.edu,
oliver@marine.rutgers.edu, reinfelder@envsci.rutgers.edu)

Moline, M.A.

California Polytechnic State University, San Luis Obispo, CA, 93407, USA (mmoline@calpoly.edu)

Zhou, M.; Chen, R.F.

University of Massachusetts Boston, Earth and Ocean Sciences, 100 Morrissey Blvd, Boston, MA, 02125, USA
(meng.zhou@umb.edu, bob.chen@umb.edu.)

Abstract- Rivers that flow through urban watersheds represent major conduits for the transport of anthropogenically derived nutrients and chemical contaminants to the coastal ocean. The fate of these materials is controlled not only by the physical dynamics of the riverine plume as it moves over the coastal shelf, but also by associated biological and chemical processes. The resulting interactions are complex and often difficult to capture using traditional oceanographic methods and resources. The advent of coastal observation systems, however, enables ocean scientists to react quickly and adaptively sample dynamic coastal environments to more fully understand key physical, chemical and biological processes. In April 2005, during the Lagrangian Transport and Transformation Experiment (LaTTE), nutrient-laden water discharged from the Hudson River was retained nearshore in a recirculating eddy before moving southward along the New Jersey coast and mixing with relatively saline coastal water. Biological sampling of the recirculating zone and southward moving plume water was facilitated by a shelf-wide coastal observatory system. Rapid nutrient uptake and assimilation by phytoplankton within the eddy resulted in extremely high rates of productivity ($> 10 \text{ mg C m}^{-3} \text{ h}^{-1}$). Approximately 75% of the fixed carbon within the eddy could be attributed to phytoplankton in the $> 20 \text{ um}$ size class determined subsequently to be comprised primarily of large ($\sim 200 \text{ um}$) chain forming diatoms. Characterization of the zooplankton assemblage revealed a dominance of small copepods, approximately 200-400 um in size, and shipboard grazing experiments indicated a negligible feeding impact of these mesozooplankton on the phytoplankton. The apparent mismatch in size between

producers and consumers, coupled with the high rates of primary production, resulted initially in a pronounced accumulation of phytoplankton biomass ($> 25 \text{ ug L}^{-1} \text{ chl a}$) within the recirculation zone with subsequent declines in dissolved oxygen concentration in bottom waters coincident with nutrient reduction and bloom senescence.

I. INTRODUCTION

Worldwide, continental shelves comprise only about 10% of the total ocean area. However, these areas which include both estuaries and shallow coastal waters account for the vast majority of primary productivity and support the largest fisheries. Of concern are the effects of a wide range of human activities on the ecological health and integrity of coastal waters, e.g., increased delivery of nutrients and other contaminants, increased fishing pressure and introductions of exotic and/or invasive species. For example, increased nutrient inputs which are often synonymous with coastal eutrophication can alter microbial community dynamics and lead to longer-term changes in both the biological and chemical characteristics of specific systems. Such changes, if left unchecked, can have catastrophic consequences, e.g., loss of economically important fisheries, production of extremely potent green house gases, altered food webs and a potential loss of biological diversity. These changes reflect both local pressures and global changes to the ocean-climate system. Therefore it is not surprising that the U.S. Commission on Ocean Policy, stated the need for "sound science for wise decisions" to ensure the sustainable use of our coastal oceans for this and future generations. The Commission also highlighted the need for, "a robust infrastructure of cutting edge technology that forms the backbone of modern ocean and coastal science and effective resource management and enforcement". It was against this backdrop, that the Rutgers Coastal Ocean Observation Laboratory (COOL) evolved. Here we describe an ocean observatory and illustrate the ability of the observatory to enable biological

research in the coastal ocean. Our focus is on data collected as part of the National Science Foundation's Langragian Transport and Transformation Experiment (LaTTE), a multidisciplinary effort to examine processes that control the fate and transport of nutrients and chemical contaminants in the Hudson River plume.

II. THE OBSERVATORY AND EXPERIMENT

As part of the the Langragian Transport and Transformation Experiment (LaTTE), multiple ships were employed to characterize the dynamics of the Hudson River buoyant plume and determine the fate of associated materials as water flowed onto the Mid-Atlantic Bight (MAB) (Fig. 1). Although, LaTTE is a multi-year effort, we pay particular attention to data collected during 2005. The field effort in 2005 was preceded by a significant Hudson outflow, the largest in 30 years, associated with the spring thaw of winter snow and a series of early spring precipitation events (Fig. 2). Field efforts were carried out at the end of the high discharge period. The buoyant plume carried significant concentrations of dissolved and particulate material that were readily visible in satellite imagery (Fig. 3).

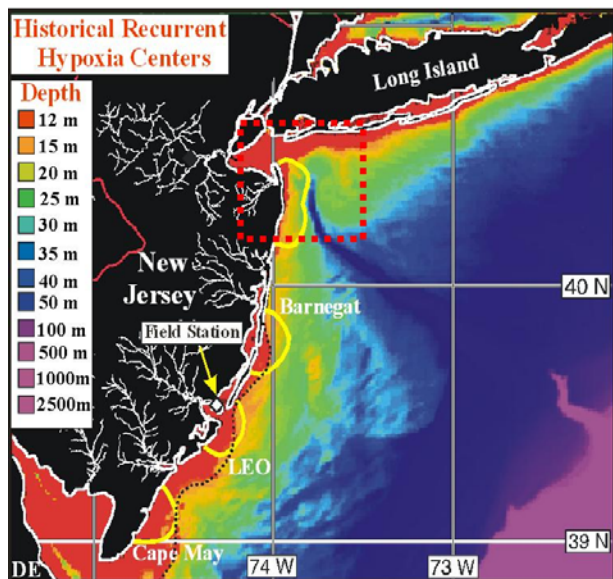


Figure 1. The location of the LaTTE was conducted along the coast of New Jersey. The red box outlines the region where field efforts were focused. The yellow lines indicate region of recurrent hypoxia/anoxia. The colors indicate the sea floor bathymetry.

The ships sampled the plume adaptively by accessing real time data collected by the New Jersey Shelf Observing System (NJ SOS) [1]. The observatory data includes: A) real-time access to the international constellation of ocean color satellites, B) a triple-nested HF CODAR radar network, C) a series of fixed location moorings and D) a fleet of Webb Slocum gliders. Ship to shore communication was maintained through a wireless communication grid [2]. The observatory data was used to direct the ships. At each station, vertical profiles of temperature ($^{\circ}\text{C}$), salinity, chlorophyll a fluorescence (converted to $\mu\text{g/L}$) and dissolved oxygen (mL/L) were taken with a Seabird SBE CTD, Wetlabs WetStar fluorometer and a

SBE oxygen sensor. Each of the aforementioned profiles was complemented with a second profile taken with a cage

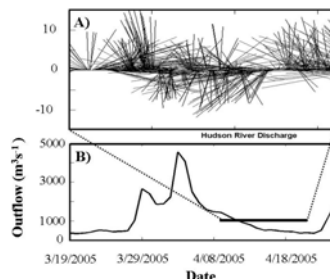


Figure 2. The wind and river discharge before, during and after the LaTTE 2005 field campaign.

outfitted with bio-optical instrumentation including an absorption attenuation meter (ac9) and 2 Wetlabs ECO-VSF systems. The real-time data allowed specific depths to be targeted and water samples were collected using Niskin bottles. Phytoplankton were subsequently quantified microscopically and also

using High Performance Liquid Chromatography. Particulate organic carbon and nitrogen were measured on discrete samples using a Carla Erba Elemental Analyzer. Size fractionated phytoplankton productivity rates were measured onboard the ship using carbon-14 radio-isotope techniques.

III. PLUME DYNAMICS

The LaTTE experiment was conducted 7 days after river outflow peaked ($\sim 4500 \text{ m}^3 \text{ s}^{-1}$) during spring 2005 following a period of substantial rains and subsequent snow melt (Fig. 2). The outflow and its ensuing decline during the field effort were evident in satellite imagery during which time the areal extent and the turbidity of the river waters declined in the coastal ocean (Fig. 3). The waters with the highest absorption were observed inside the bays with lower values observed offshore (Fig. 3). Differences in the optical properties of the Raritan

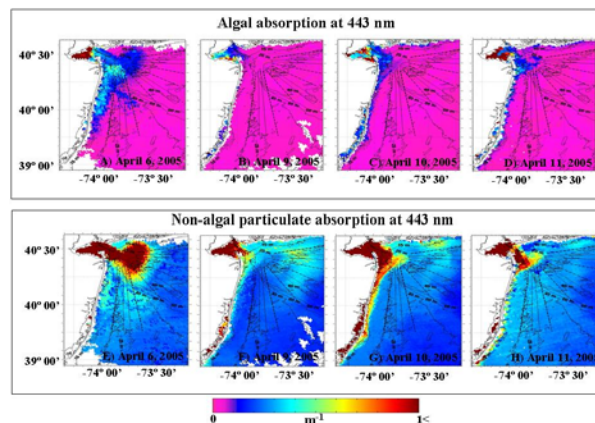


Figure 3. Satellite derived estimates of phytoplankton and non-algal particulate material. The ocean color imagery was processed using a multi-band quasi-analytical algorithm that estimates the absorption and backscattering coefficients [3]. The total absorption estimated is inverted into phytoplankton pigments and non-algal absorption.

and Hudson rivers were evident in the ocean color imagery (Fig. 3). Both rivers had high concentrations of non-algal particle absorption, but the Raritan waters exhibited higher phytoplankton absorption than the Hudson River (Fig. 3).

During the 2005 field effort, winds were variable (Fig. 2) and impacted the dynamics of the river plume. During the first five days of the field effort, winds were largely from the north with periods of sustained winds of $>10 \text{ ms}^{-1}$. Winds then reversed to south and were complemented with afternoon sea breezes. The southerly and sea breeze winds resulted in river waters forming a bulge of turbid freshwater at the mouth of the estuary that showed significant recirculation before it flowed to the south along the New Jersey coast (Fig. 4). The bulge formation during this event was definitive because strong upwelling winds on April 6-8th cleared the region of a previous outflow by driving the freshwater to the east along the Long Island coast and upwelling saline water along New Jersey (Fig. 3). Winds shifted to downwelling on April 8 and a new plume emerged. Because the outflow was clearly distinct from the older plume to the east, we were able to observe its evolution in detail. While the new outflow did set up a coastal current, as evident by both the absorption characteristics and the sequential drop in salinity at the inshore moorings (Fig. 5), estimates of fresh water fluxes in the coastal current made with both the moored instruments and ships indicated that only approximately 1/3 of the outflow became incorporated into the coastal current, while the remaining 2/3 of outflow contributed to the bulge growth. Independent estimates of fresh water volume in the bulge on April 14th based on shipboard data (Fig. 6) suggested a mean freshwater flux into the bulge of approximately $2300 \text{ m}^3 \text{ s}^{-1}$. The sum of freshwater fluxes we estimated going into the bulge and into the coastal current is close to the measured discharge in the river.

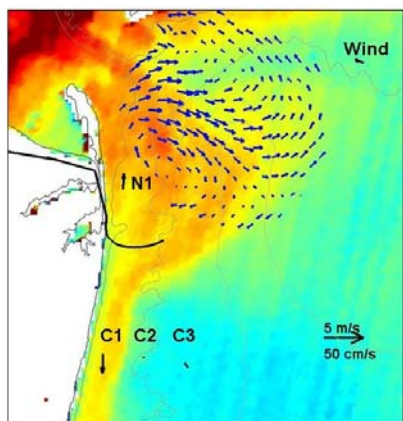


Figure 4. Mean surface currents from CODAR and moored data from April 11th overlaid on a remotely sensed map of chlorophyll *a* measured with the Indian OCM satellite. The thick black line is drifter trajectory (track on the land reflects the drifter track is in a graduate student's truck after recovery when it washed up on the beach)

east, we were able to observe its evolution in detail. While the new outflow did set up a coastal current, as evident by both the absorption characteristics and the sequential drop in salinity at the inshore moorings (Fig. 5), estimates of fresh water fluxes in the coastal current made with both the moored instruments and ships indicated that only approximately 1/3 of the outflow became incorporated into the coastal current, while the remaining 2/3 of outflow contributed to the bulge growth. Independent estimates of fresh water volume in the bulge on April 14th based on shipboard data (Fig. 6) suggested a mean freshwater flux into the bulge of approximately $2300 \text{ m}^3 \text{ s}^{-1}$. The sum of freshwater fluxes we estimated going into the bulge and into the coastal current is close to the measured discharge in the river.

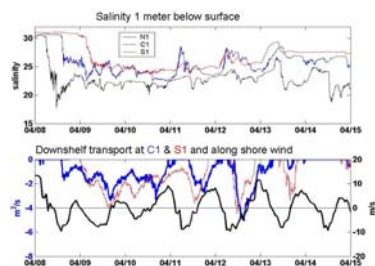


Figure 5. (A) Surface salinity at three mooring sites along New Jersey (sites N1, C1 and S1). Note high salinity prior to 4/8 at all moorings is at salinity values >30 . (B) Down shelf transport in coastal current (color) and alongshore winds (black).

approximately $2300 \text{ m}^3 \text{ s}^{-1}$. The sum of freshwater fluxes we estimated going into the bulge and into the coastal current is close to the measured discharge in the river.

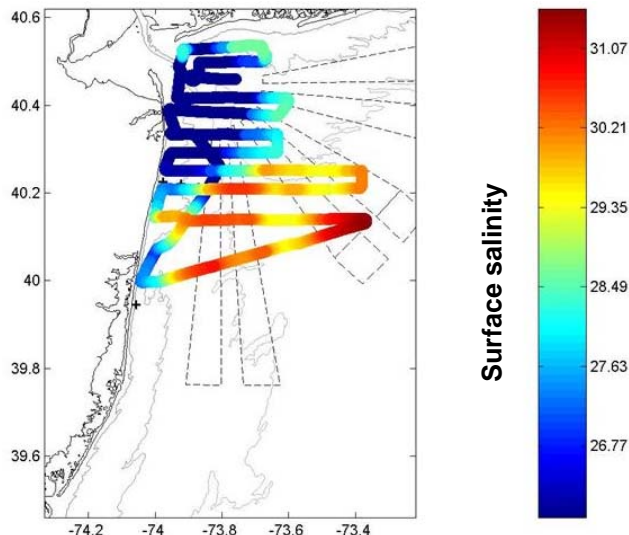


Figure 6. Bulge clearly identified by surface salinity from survey April 13-15. Using CTD profiles collected with a towed undulating shuttle, we estimated the bulge accumulated 1.2 billion cubic meters since April 8th.

III. THE CHEMISTRY AND BIOLOGY OF THE PLUME

The bulge is a mixture of new water entering it and the older recirculating water. Thus, the water that enters the coastal current at the southern edge of the plume is also a mixture of new and old water. Both the age of the fluid in the bulge and fluid in the coastal current are qualitatively reflected in the evolution of nitrate concentration in the region (Fig. 7). Nitrate concentrations near Sandy Hook at the outflow were 15-20 $\mu\text{M/L}$ both on April 9th shortly after the commencement of bulge formation and 6 days later on April 15th, indicating that for constant outflow the input of nutrients to the bulge would be constant over time. However, within the bulge nitrate concentrations decreased from 10-15 $\mu\text{M/L}$ to 5-10 $\mu\text{M/L}$ over the 6 day period, while salinity in the bulge remained relatively

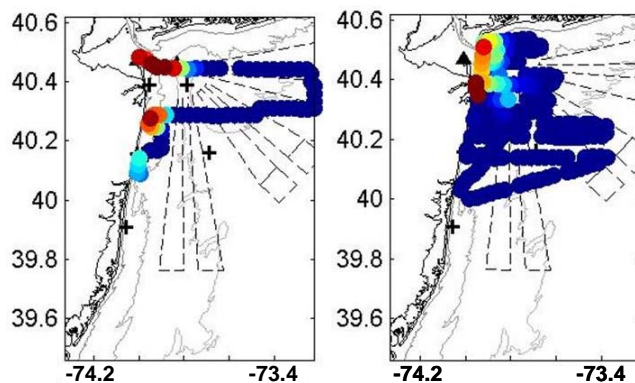


Figure 7. Surface maps of nitrate on (A) 4/10/2006 and (B) 4/14/2006. The nitrate concentrations range from 0 to 15 mM L^{-1} . Note the downshelf penetration of NO_3 on 4/10/2006 is absent on 4/14/2006.

constant. Furthermore, higher nitrate concentrations penetrated downshelf in the coastal current on April 10th where they exceeded 5 $\mu\text{M/L}$ at 40.1 N, while during the April 13-15, nitrate concentrations were nearly zero along the coast. This indicates the initial coastal current contained nutrient rich

waters that recently exited New York Harbor reflective of the young age of the fluid in the new bulge. As the water aged, nutrient concentrations decreased markedly due to rapid uptake and assimilation by phytoplankton that drove the intense productivity we observed. By the end of this period (April 15th), the water had aged sufficiently that very little nitrate was delivered to the southward flowing coastal current, i.e. the majority of the nitrate removal occurred in the bulge region within the New York Bight Apex. The rapid mixing and retention of fluid in the bulge was evident in the patterns of drifter movement; drifters were released on an ebb tide coincident with the introduction of new water into the bulge (Fig. 4). Drifters released on April 11th into water that exited the harbor several hours earlier did not join the coastal current to the south, but rather remained in the recirculating bulge veering back toward the shore (Fig. 4). These results agreed with dye that was injected into the plume which spread into an elongated patch with a length scale on the order of the bulge itself within 24 hours after injection (Houghton personnel communication).

Phytoplankton concentrations were high within the low salinity waters of the buoyant river plume. Chlorophyll *a* concentrations were highest in the low salinity waters with concentrations in the plume exceeding 60 mg m⁻³ (Fig. 8a). In contrast the chlorophyll *a* concentrations in marine waters were often less than 5 mg m⁻³ (Fig. 8a). The chlorophyll *a* concentrations were highly correlated with fucoxanthin ($R^2 = 0.96$) indicating that diatoms dominated these waters (Fig. 8b).

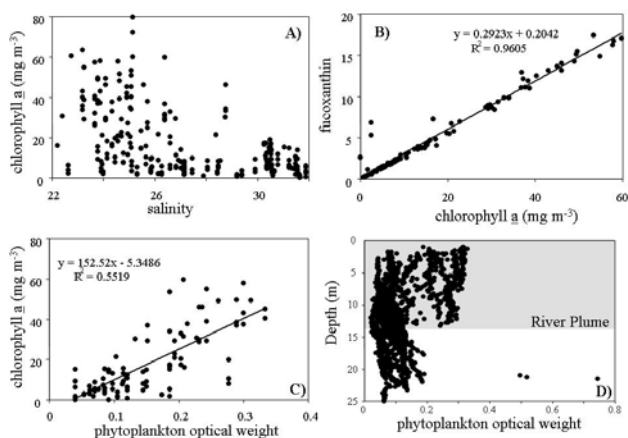


Figure 8. (A) The variability of chlorophyll *a* (mg m⁻³) versus salinity. (B) The correlation between the chlorophyll *a* versus that of fucoxanthin (units). (C) The significant correlation ($p < 0.05$) between chlorophyll *a* and phytoplankton optical weight derived from ac9 data. (D) The depth dependent distribution of phytoplankton optical weight as a function of depth. The grey box delineates the depths associated buoyant plume. The phytoplankton weights are significantly higher in the buoyant surface plume.

Alloxanthin was the one chemotaxonomic pigment that was also correlated with both fucoxanthin ($R^2 = 0.38$) and chlorophyll *a* ($R^2 = 0.42$) indicating cryptomonads were also present. No other chemotaxonomic pigments were correlated with chlorophyll *a*. Chlorophyll *a* concentrations were

positively with the phytoplankton optical weights ($R^2 = 0.55$, $p < 0.05$) estimated from the ac-9 measurements (Fig. 8c) and the increased absorption of phytoplankton was clearly evident in the buoyant surface waters (Fig. 8d).

The colored optical constituents showed distinctive patterns that were associated with the Hudson river plume. Overall, the optical concentration of phytoplankton was linearly correlated ($R^2 = 0.75$) with non-algal particle and colored dissolved organic material (CDOM) absorption (Fig. 9a). While the absolute concentrations of optical material were linearly correlated, the relative contribution of colored material was variable within the water masses. CDOM optical weights were negatively correlated with salinity ($R^2 = 0.81$) to about a salinity of 28 (Fig. 9b). At salinities higher than 28 salinity units, CDOM optical weights exhibited no relationship with salinity (Fig. 9b). In contrast, within low salinity waters (< 28 salinity units), the relative contribution of phytoplankton to total absorption (at 676 nm) was relatively constant at 70% (Fig. 9c). At salinities higher than 28, the relative contribution of phytoplankton absorption was variable. Relatively low phytoplankton concentrations were often associated with oceanic bottom waters with the low phytoplankton

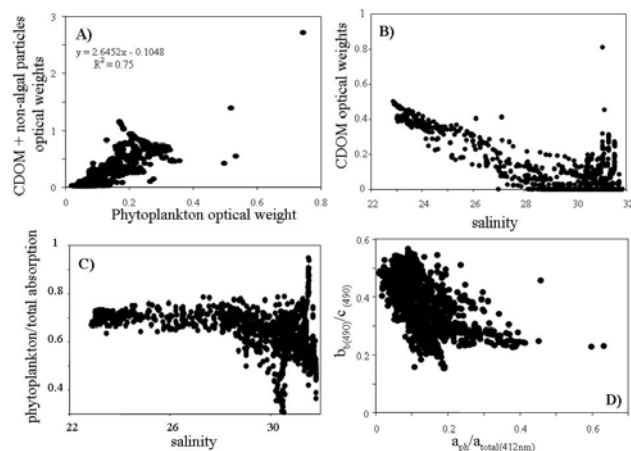


Figure 9. (A) The correlation between phytoplankton optical weight and combined CDOM and nonalgal phytoplankton optical weight estimated from the ac9 measurements. (B) The inverse correlation between the optical weight of CDOM and salinity. The inverse relationship is robust until salinity values exceed 28 salinity units. At the salinity values greater than 28 salinity units, the CDOM optical weight values shows no correlation with salinity. (C) The proportion of the total absorption associated with phytoplankton versus salinity. (D) The ratio of backscatter to total attenuation versus the proportion of total absorption

concentrations and were dominated by nepheloid layers comprised largely of detritus and CDOM. High salinity surface waters had relatively high concentrations of phytoplankton associated with surface blooms. The waters with relatively high phytoplankton absorption were inversely correlated to the ratio of backscatter to total attenuation (Fig. 9d) suggesting that particles were larger and/or more minerogenic in the waters with relatively low phytoplankton absorption.

The optical properties within the plume were dynamic reflecting the dynamics of CDOM, detritus and phytoplankton (Fig. 10). River waters near the mouth of the Hudson were turbid with high concentrations of phytoplankton, CDOM, and detritus when compared to surrounding oceanic waters (compare Fig. 10A to 10E-H). In marine waters, phytoplankton represented the dominant absorbing constituent (Fig. 10E-H). In contrast, in the river waters just entering the coastal waters, CDOM had the highest absorption values approaching 0.9 m^{-1} at 440 nm (Fig. 10A). Detritus absorption was also greater than phytoplankton absorption. By the time the buoyant waters recirculated and began to flow southward along the New Jersey coast, the phytoplankton absorption had increased by 30% while detritus and CDOM values decreased by a factor of 4 (Fig. 10A-C). As the buoyant waters moved further down the New Jersey coast, all values for phytoplankton, CDOM and detritus dropped substantially; absorption magnitudes were $< 0.1 \text{ m}^{-1}$ (Fig. 10D).

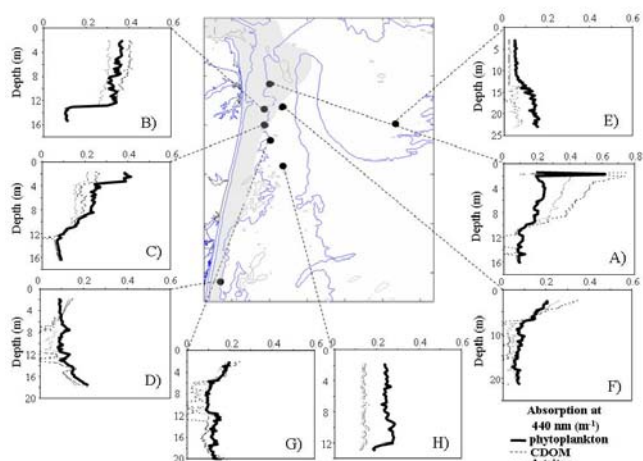


Figure 10. The spatial and depth-dependent variability in the colored constituents within the Hudson River plume. The colored constituents include phytoplankton, CDOM, and nonalgal particulates. The colored components are estimated by inverting ac9 data [4].

The observed dynamics of the phytoplankton absorption within the plume were confirmed with size fractionated radio-isotope measurements. The buoyant plume was extremely productive with carbon fixation rates exceeding $10 \text{ mg C m}^{-3} \text{ hr}^{-1}$ (Fig. 11). Phytoplankton carbon fixation rates within the bulge were dominated by large cells with the greater than $20 \mu\text{m}$ size fraction accounting for 70% of the carbon fixation (Fig. 11A). The phytoplankton communities were dominated by chain forming diatoms (e.g., *Skeletonema costatum*). The actual size of the chain forming diatoms were significantly greater than $20 \mu\text{m}$, with some chains exceeding $200 \mu\text{m}$ in length. Cells in the 2-20 and the 0.2-2 μm size fraction accounted for 17% and 13% of phytoplankton productivity, respectively (Fig. 11A). High productivity rates were correlated with the high chlorophyll concentrations, particulate organic carbon and phytoplankton absorption. As a consequence of high productivity and low grazing impact, there was an accumulation of phytoplankton biomass ($> 25 \mu\text{g L}^{-1} \text{ chl a}$) within the

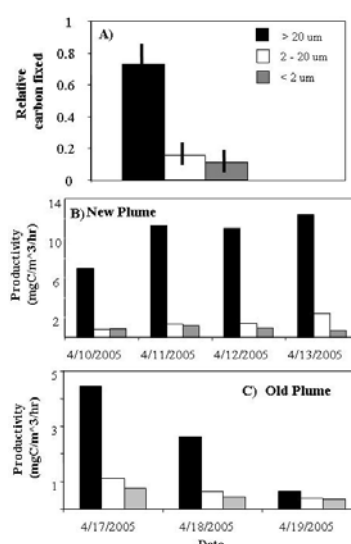


Figure 11. The size fractionated phytoplankton productivity. A) The average proportion of the phytoplankton productivity for the entire LaTTE 2005 database B) and C) The time course change in size fractionated phytoplankton productivity in the Hudson river bulge.

recirculation zone. Subsequent declines in dissolved oxygen concentration in bottom waters were attributed to nutrient reduction and bloom senescence. As waters within the plume aged, both phytoplankton productivity and the relative contributions of the different size fractions changed presumably as a consequence of a decrease in nutrients within the recirculating bulge (Fig. 11B, C). In fact, total productivity decreased by almost 5-fold, due largely to the declining productivity in the $>20 \mu\text{m}$ cell fraction. The declines in productivity within the buoyant plume were mirrored by declines in the nitrogen concentrations (Fig. 7).

Oxygen concentrations and percent saturation values were highly variable in these waters. In surface waters, the oxygen concentrations were supersaturated with percent saturation values sometimes exceeding 140% (Fig. 12). Supersaturated values were found in low salinity waters where phytoplankton biomass and productivity rates were high (Fig. 11). In contrast, the high salinity bottom waters beneath the buoyant plume were under-saturated in oxygen with values dropping to 70% of saturation (Fig. 12). Particulate organic carbon concentrations in the buoyant plume were as high as 0.4 mg C

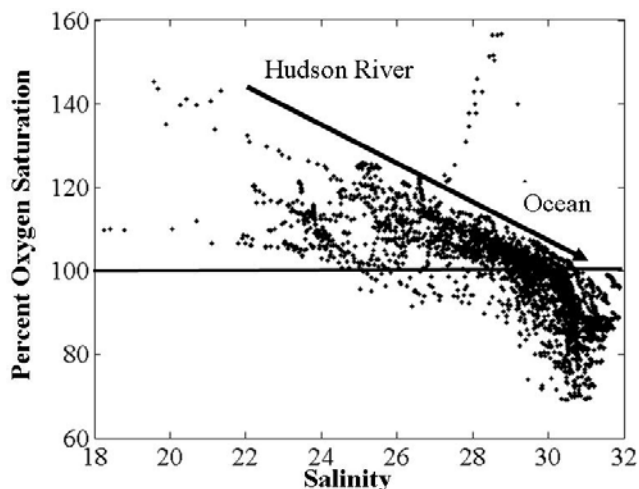


Figure 12. The inverse relationship between salinity and the percent oxygen saturation within the LaTTE experimental region in spring 2005. The most saline waters reflect bottom waters under the buoyant plume.

ml⁻¹. Characterization of the zooplankton assemblage revealed a dominance of small copepods, approximately 200-400 μm in size, and shipboard grazing experiments indicated a negligible feeding impact of these mesozooplankton on the phytoplankton. The producers and consumers, coupled with the high rates of primary production, resulted initially in a pronounced accumulation of phytoplankton biomass (> 25 μg L⁻¹ chl *a*) within the recirculation zone with subsequent declines in dissolved oxygen concentration in bottom waters coincident with nutrient reduction and bloom senescence.

Using the depth of the plume, growth rates of phytoplankton within the plume, range of days of recirculation within the plume, the sources (river), and the sinks (river exiting the

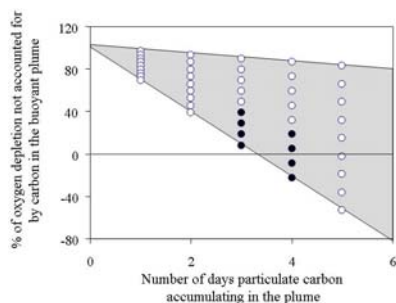


Figure 13. The amount of oxygen depletion that could be accounted for by the particulate organic carbon in the surface waters and the retention time within the Hudson river bulge. The blackened circles indicate the range of conditions observed during LaTTE. The range (circles) for each day retained in the plume reflects the impact of the depth of the plume (ranging from 1 to 9 m deep) on the oxygen depletion.

IV. OXYGEN DEPLETION ALONG THE NEW JERSEY COAST

In 1976, a widespread decline in bottom water dissolved oxygen (DO) resulted in hypoxic/anoxic conditions over the entire Mid Atlantic Bight (MAB) continental shelf [5]. The declines in oxygen were associated with a larger than normal river runoff during a warm winter that resulted in early stratification of the MAB. This sequence of events resulted in a large phytoplankton bloom that exported carbon into the bottom waters which fueled the depletion of oxygen [6]. This event, and the associated economic losses, prompted the initiation of long-term DO monitoring in the MAB [7] which documented four 30 by 30 kilometer recurrent regions of hypoxia/anoxia along the New Jersey coast (Fig. 1). In these regions, nearly one third of the summer bottom water data from 1977-1985 had hypoxic conditions with reduced oxygen concentrations in the bottom water inshore of the 20 m isobath [8]. The close proximity to specific rivers and estuaries lead to the hypothesis that anthropogenic loading of organic matter fueled the declines in bottom water DO [9-10]; however this hypothesis had problems as several relatively pristine rivers had low DO zones while other anthropogenically impacted

rivers did not. Upwelling was hypothesized as another mechanism that could drive these recurrent regions of low DO along New Jersey.

Variations in ocean temperatures along the New Jersey coast (1-4 degrees), other than seasonal mixing, are caused by episodic summer upwelling events driven by SW winds associated with the Bermuda High [1, 11]. During the 1990's, the New Jersey coast averaged 37 days of upwelling in the summer months [11]. Off the southern coast of New Jersey, topographic variations associated with ancient river deltas promote upwelled water, which is initially a feature along the entire NJ coast, to evolve into an alongshore line of recurrent upwelling centers [12] that are co-located with several of the historical regions of low dissolved oxygen and provide sufficient organic matter to deplete bottom water DO [11]. While this upwelling mechanism can explain 3 of the 4 recurrent low DO zones, it does not explain the fourth low DO zone at the southern edge of the Hudson River. The results from LaTTE suggest high algal productivity near the mouth of the Hudson River is likely to account for recurrent observations of low oxygen in this area.

V. REFERENCES

- [1] Schofield, O. et al. "Linking regional coastal observatories to provide the foundation for a national ocean observation network" *J. Oceanic Eng.* 27(2): pp. 146-154, 2002.
- [2] Glenn, S. M., Schofield, O. "Observing the oceans from the COOLroom: Our history, experience, and opinions" *Oceanogr.* 16(4): 37-52, 2003.
- [3] Lee, Z., Carder, K. L., Arnone, R. A. "Deriving inherent optical properties from water color: a multiband quasi-analytical algorithm for optically deep waters" *Appl. Optics* 41: 5755-5772, 2002.
- [4] Schofield, O. et al. "Inverting inherent optical signatures in the nearshore coastal waters at the Long Term Ecosystem Observatory" *J. Geophys. Res.* VOL. 109, C12S04, DOI:10.1029/2003JC002071, 2004
- [5] Figley, W. B Pyle, and B. Halgren " Socioeconomic impacts, in Oxygen Depletion and Associated Benthic Mortalities in New York Bight, 1976" NOAA Prof. Pap. 11, edited by R. L. Swanson and C. J. Sindermann, Natl. Oceanic and Atmos. Admin., Silver Spring, Md., pp. 315 – 322, 1979.
- [6] Falkowski, P. G., T. S. Hopkins, and J. J. Walsh "An analysis of factors affecting oxygen depletion in the New York Bight" *J. Mar. Res.* 38, 479–506, 1980.
- [7] Atwood, D. K., et al. "Chemical factors, in Oxygen Depletion and Associated Benthic Mortalities in New York Bight, 1976" NOAA Prof. Pap. 11, edited by R. L. Swanson and C. J. Sindermann, , Natl. Oceanic and Atmos. Admin., Silver Spring, Md., pp. 79– 123, 1979
- [8] Stoddard, A., J. E. O'Reilly, T. E. Whitedge, T. C. Malone, and J. F. Malone "The application and development of a compatible historical data based for the analysis of water quality management issues in the New York Bight" *IEEE*, 1030– 1035, 1986
- [9] Steimle, F. "Dissolved oxygen levels in York Bight waters during 1977" NOAA Tech. Memo. NMFS-NE 20, N. E. Fish. Cent., Woods Hole, Mass., 1978.
- [10] Warsh, C. "NOAA's Northeast Monitoring Program (NEMP): A report on progress of the first five years (1979– 84) and a plan for the future" NOAA Tech. Memo. NMFS-F/NEC-44, N. E. Fish. Cent., Woods Hole, Mass., pp. 9 – 20, 1987.
- [11] Glenn, S. M. et al. " Biogeochemical impact of summertime coastal upwelling on the New Jersey Shelf" *J. Geophys. Res.* 109 C12S02, DOI:10.1029/2003JC002265, 2004.
- [12] Song, Y. T., D. B. Haidvogel, and S. M. Glenn. "Effects of topographic variability on the formation of upwelling centers off New Jersey: A theoretical model." *J. Geophys. Res.* 106 (C5):9223-9240, 2001.